A&A 433, L49–L52 (2005)
DOI: 10.1051/0004-6361:200500093

Astronomy & Astrophysics

Detection of γ-ray lines from interstellar ^{60}Fe by the high resolution spectrometer SPI

M. J. Harris[1], J. Knödlseder[1], P. Jean[1], E. Cisana[2], R. Diehl[3], G. G. Lichti[3], J.-P. Roques[1], S. Schanne[4], and G. Weidenspointner[1]

[1] Centre d'Étude Spatiale des Rayonnements, BP 4346, 31028 Toulouse Cedex 4, France
e-mail: Mike.Harris@cesr.fr
[2] IASF, via E. Bassini 15, 20133 Milano, Italy
[3] Max-Planck-Institut für extraterrestrische Physik, Postfach 1603, 85740 Garching, Germany
[4] DSM/DAPNIA/SAp, CEA Saclay, 91191 Gif-sur-Yvette, France

Received 1 February 2005 / Accepted 23 February 2005

Abstract. It is believed that core-collapse supernovae (CCSN), occurring at a rate ∼once per century, have seeded the interstellar medium with long-lived radioisotopes such as ^{60}Fe (half-life 1.5 Myr), which can be detected by the γ-rays emitted when they β-decay. Here we report the detection of the ^{60}Fe decay lines at 1173 keV and 1333 keV with fluxes $3.7 \pm 1.1 \times 10^{-5}$ γ cm^{-2} s^{-1} per line, in spectra taken by the SPI spectrometer on board *INTEGRAL* during its first year. The same analysis applied to the 1809 keV line of ^{26}Al yielded a line flux ratio ^{60}Fe/^{26}Al $= 0.11 \pm 0.03$. This supports the hypothesis that there is an extra source of ^{26}Al in addition to CCSN.

Key words. ISM: abundances – nucleosynthesis – gamma-rays: observations

1. Introduction

The radioactive isotopes ^{26}Al and ^{60}Fe are both believed to be produced in massive stars that end their lives as core collapse supernovae (CCSN; masses $> 8M_{\odot}$). Further, they have similar half-lives (7.4×10^5 yr and 1.5×10^6 yr respectively) which are much longer than the characteristic interval between CCSN (∼100 yr). Therefore they will accumulate in the interstellar medium until a steady state is reached, and indeed this steady-state abundance of ^{26}Al has been detected via a flux $\sim 4 \times 10^{-4}$ γ cm^{-2} s^{-1} in the 1809 keV line from its β-decay (Mahoney et al. 1982; Diehl 2001).

The sky distribution of ^{26}Al has been mapped (Knödlseder et al. 1999) and, as expected, the line emission is dominated by the Galactic plane, where massive stars are found. It might be expected that the distribution of ^{60}Fe line emission (at 58 keV, 1173 keV and 1333 keV) would be very similar. However (as we will see in Sect. 4) there are subtle differences in the sources of the two isotopes (mass and metallicity of star, depth within star and effect of the final explosion) which make the relative distributions of ^{60}Fe and ^{26}Al a potential source of information on fine details of massive-star evolution.

In this paper we report the detection of two of the ^{60}Fe lines by the SPI instrument, part of the *INTEGRAL* mission. The significance of this detection is not sufficient for us to draw any conclusions about the sky distribution relative to ^{26}Al. However the mission is expected to continue for several years, by which time there may be enough data for spatial information to be extracted. Earlier measurements (summarized by Harris et al. 1997) did not detect ^{60}Fe, and yielded only upper limits on the ^{60}Fe/^{26}Al ratio, until the preliminary detection reported by *RHESSI* (Smith 2004), which is consistent with ours (Sect. 3.4).

2. Observations and analysis

The *INTEGRAL* spacecraft was launched October 17, 2002 into a high-inclination, high-eccentricity orbit with a 3-day period. It carries two major γ-ray instruments, the co-aligned IBIS and SPI. Although each performs both imaging and spectroscopic tasks, IBIS is designed for fine spatial resolution while SPI has superior energy resolution. Its 19 Ge detectors achieve ∼0.3% resolution around 1 MeV; imaging at the level ∼3° within a 16° × 16° field is enabled by a coded mask permitting differential illumination of the detectors as a function of angle. In our analysis we do not make use of this capability, because of the weakness of the lines.

One input into our analysis is therefore an assumption about the Galactic distribution of ^{60}Fe. We used the distribution of far-infrared (240 μm) emission mapped by *COBE*/DIRBE (Hauser et al. 1998) which is expected to be a good guide to the distribution of massive stars and is in fact one of the best predictors of ^{26}Al emission (Knödlseder et al. 1999).

The observations available for use in our analysis were made during the first year of operations (orbits 19–130) and largely came from two core (instrument team) programmes – two deep exposures (4 Ms) to the Galactic centre, and a periodic scan along the Galactic plane. We also made use of data publicly released as of 2004 December. This amounted to 13.5 Ms distributed over the whole sky, but favouring the inner Galaxy locations where the DIRBE 240 μm and COMPTEL ^{26}Al maps and the massive star population peak (see e.g. the exposure map of Knödlseder et al. 2005).

During orbits 19–130 SPI's performance was nominal, with all 19 detectors operating at full efficiency (effective area 70 cm^2) and resolution (2.5 keV *FWHM* at 1.3 MeV). The energy resolution was maintained against the degradation caused by cosmic-ray impacts by in-orbit annealing, which was effective in restoring performance. In our analysis we allowed for the fact that comparisons between spectra taken at different epochs would have found slightly different widths and energies for the same line, due to this time variability of resolution (Sect. 3.2). Similarly, we analyzed separately single-detector events (SE) and "multiple" events (ME) where the γ-ray energy was deposited in two detectors because their effective spectral resolution and instrumental backgrounds differ somewhat.

The basic principle behind our analysis was the creation of models describing the time variation of the background count rates, which dominate the cosmic signal by a factor ∼100. The models were made up from physically plausible environmental quantities that ought to contribute to the background. Empirically, the prompt component of the background (both line and continuum) is well described by the count rates in the Ge detectors when saturated (energy loss >8 MeV, hereafter "GEDSAT" rates). But the prompt interactions also create radioactive isotopes with finite half lives, which are strong sources of background lines. The most important example is radioactive ^{60}Co, which decays with a 7.6-year mean life emitting two γ-ray lines identical with those from cosmic ^{60}Fe. We modelled this time series by convolving the source term (GEDSAT) with an exponential increasing on a 7.6 yr time scale. We define the term *template* to mean a function of environmental variables whose time series we will fit to the background data, whether simple (like GEDSAT) or complex (such as GEDSAT ⊗ 7.6 yr). If there is a cosmic source of the lines, it should follow a quite different time series (SPI's successive exposures to the 240 μm map), so we make this the third term in the fit.

The best results were obtained when all three components (two background templates and the expected ^{60}Fe flux) were fitted simultaneously to the count rates by detector and pointing in 1 keV bins (Sect. 3.1). We performed an alternative analysis in which the "off-pointings" which are empty of ^{60}Fe according to the 240 μm map were treated separately (Sect. 3.2). The results of this are used only as a check, and are not included in our final result, since they contain several systematic errors. Finally, since the cosmic ^{60}Fe/^{26}Al ratio is perhaps the most interesting quantity which we can derive, we have analysed the 1.809 MeV line of ^{26}Al in the identical way, so as to eliminate systematics from the ratio if possible (Sect. 3.3).

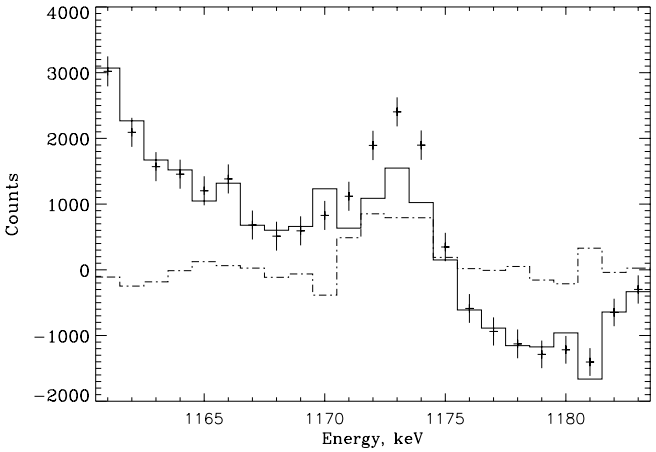

Fig. 1. Amplitudes of the GEDSAT background term (full line) and the GEDSAT ⊗ 7.6 yr background term (dot-dash line) fitted (along with the ^{60}Fe map exposure) to the time series of SE count rates for 1161–1184 keV. Data points – background counts in 1 keV bins with flat continuum subtracted.

3. Results and evaluation

3.1. The templates fitted to all pointings simultaneously

In this analysis the count rates in the ^{60}Fe lines were measured as described below in each of the 6821 pointings in our data set, and fitted by the templates GEDSAT and GEDSAT ⊗ 7.6 yr, and by the expected cosmic ^{60}Fe flux (i.e. SPI's exposure to the 240 μm map). A template for the continuum which consisted of GEDSAT convolved with the time series of count rates summed over two bands on either side of each line (1163–1169, 1177–1183 keV, and 1318–1328, 1349–1359 keV) was kept fixed in the fit. The line count rates to be fitted were obtained by summing over the intervening intervals (avoiding blending lines as in 1335–1348 keV). The line count rates in 1 keV bins, and the best-fitting amplitudes of GEDSAT and GEDSAT ⊗ 7.6 yr, are shown for SE data in Fig. 1. Clearly the variation of the count rates away from the line is explained by high amplitudes of the GEDSAT variable, while those in the line itself are strongly influenced by the 7.6 yr time-scale in the other template, which otherwise has amplitude zero as expected.

The method thus explains the background (typically ∼99% of the total) well, and we plot the amplitudes of the ^{60}Fe term in the fit (signal-to-noise ∼1%) to get our result (Figs. 2–3). The spectra appear to be quite free of systematics, except for the strong ^{69}Ge L-shell-capture decay line at 1337 keV. A more subtle systematic error (Sect. 2) might arise in the line energies and widths in Figs. 2 and 3 from the variation of the energy resolution (due to degradation and annealing) during the period covered by the measurements, which we consider below (Sect. 3.2c and footnote 1). With this caveat we find the mean strength of each of the ^{60}Fe lines to be $3.7 \pm 1.1 \times 10^{-5}$ γ cm^{-2} s^{-1} by fitting the spectra in Figs. 2 and 3 by a model consisting of either one or two Gaussian lines of fixed

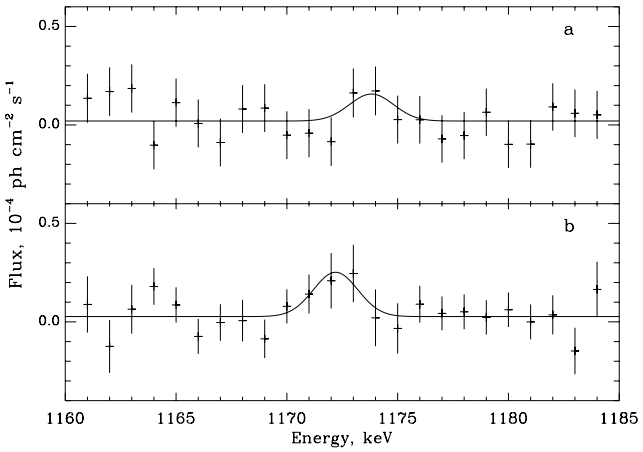

Fig. 2. Spectra of **a)** SE and **b)** ME from the analysis of Sect. 3.1, with fitted ^{60}Fe lines of strength $3.4 \pm 2.5 \times 10^{-5}$ γ cm^{-2} s^{-1} and $5.6 \pm 2.7 \times 10^{-5}$ γ cm^{-2} s^{-1} respectively.

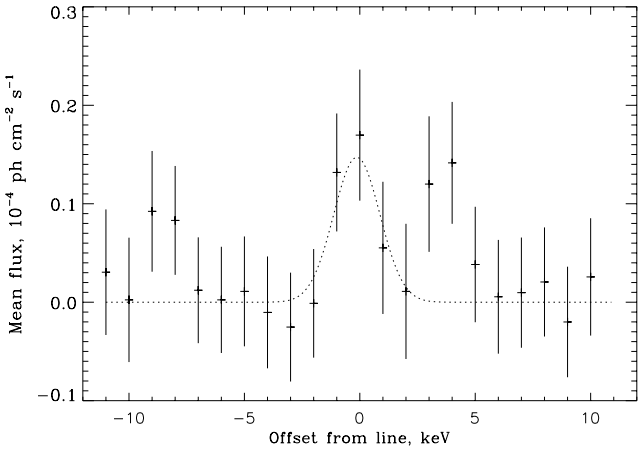

Fig. 4. Spectra of Figs. 2 and 3 overlaid and summed to give the total ^{60}Fe signal. Dotted line – the 3.7×10^{-5} γ cm^{-2} s^{-1} line deduced from combining Figs. 2a,b and 3a,b.

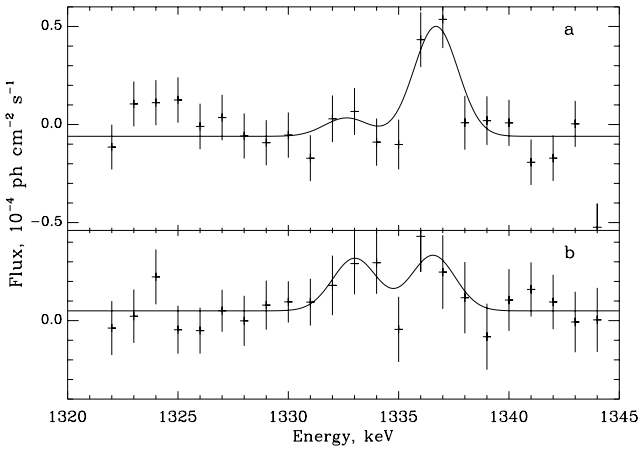

Fig. 3. Spectra of **a)** SE and **b)** ME obtained from the analysis of Sect. 3.1, with fitted ^{60}Fe lines of strength $2.3 \pm 1.6 \times 10^{-5}$ γ cm^{-2} s^{-1} and $6.7 \pm 3.2 \times 10^{-5}$ γ cm^{-2} s^{-1} respectively. The blending ^{69}Ge decay line is also fitted.

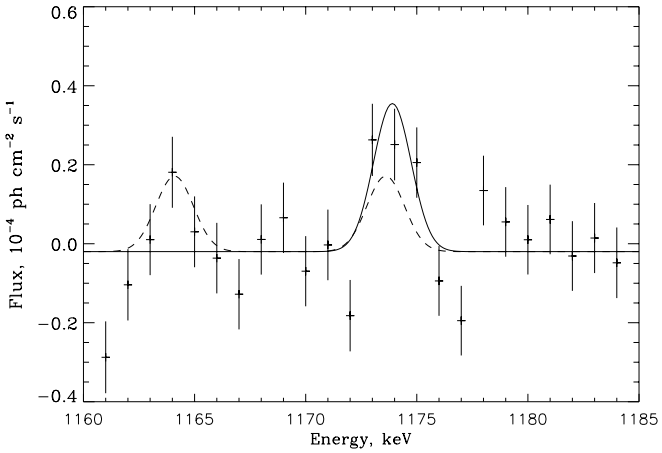

Fig. 5. Spectrum of SE obtained by the analysis of Sect. 3.2. Full line – fitted ^{60}Fe line of strength $7.9 \pm 2.1 \times 10^{-5}$ γ cm^{-2} s^{-1}. Dashed line – fitted ^{62}Ni line of strength $4.0 \pm 1.9 \times 10^{-5}$ γ cm^{-2} s^{-1} (1163 keV), and inferred line of equal strength at 1173 keV.

width 2.4 keV FWHM plus a flat continuum[1]. The significance is best visualized by summing all four lines together (Fig. 4).

3.2. The templates fitted to off-pointings

In this alternative analysis method we attempted to derive a "universal" combination of templates which describes the variation of the ^{60}Fe count rates during those pointings for which we are fairly confident that there is no signal, i.e. "off"-pointings towards Galactic latitudes >20°. Only background templates were fitted to these data. To the optimum combined template we applied a correction for the discrepancies in energy resolution due to detector degradation effects, which must exist between the off-pointings and the Galactic pointings, using the algorithm described by Knödlseder et al. (2004).

[1] The value 2.4 keV was obtained from measurements made after a correction had been applied for the variability of the instrumental energy resolution (Sect. 3.2c).

We could then obtain a measurement of the ^{60}Fe lines by fitting the fixed combination of templates and expected cosmic line strengths to the Galactic pointing data. An example of the results is shown in Fig. 5. There are clearly systematic effects due to the failure of the template to remove the time series of blending lines with various half-lives, notably ^{62}Ni (1173 keV, prompt), ^{52}Mn (1334 keV, τ = 8.066 d) and ^{69}Ge (1337 keV, τ = 2.348 d). Even the inclusion in the combined template of convolutions of these lifetimes with GEDSAT did not remove these lines. We made the following corrections for such systematic errors:

(a) The 1173 keV ^{62}Ni line by chance happens to follow immediately in the ^{62}Ni de-excitation cascade after a transition at 1163 keV which is also visible in our spectrum. The branching ratio is 100%, and the line strengths are in the ratio 1:1 if the ^{62}Ni is produced by spallation. Measuring the 1163 keV line strength immediately gives the 1173 keV line strength to be subtracted from the ^{60}Fe line (dashed line in Fig. 5).

(b) The ^{52}Mn line strength cannot be deduced as in (a), so we fitted the 1332.5 keV ^{60}Fe line under the assumptions that the ^{52}Mn line flux was either free or set to zero, the difference in the ^{60}Fe line flux being the systematic error.
(c) The effect of the correction for SPI's variable energy resolution was measured by fitting the spectra with, and without applying it. When we fixed the widths at the typical corrected value 2.4 keV, the differences between the fluxes measured were very small ($\leq 0.3 \times 10^{-5}$ γ cm^{-2} s^{-1}).

The result of this version of the analysis is 4.0 ± 1.1(stat.) $\pm$ 0.7(syst.) $\times 10^{-5}$ γ cm^{-2} s^{-1}

3.3. Measurement of the 1.809 keV line of ^{26}Al

A measurement of the 1.809 ^{26}Al line by exactly the same method as in Sect. 3.1 yielded a result $3.4 \pm 0.2 \times 10^{-4}$ γ cm^{-2} s^{-1}, for a ^{60}Fe/^{26}Al line flux ratio of 0.11 ± 0.03, corresponding to an abundance ratio 0.23 ± 0.08.

3.4. Evaluation

The close agreement between the results of the two analyses (Sects. 3.1, 3.2) suggests that the correction to the line widths and energies for the varying instrumental resolution probably has little effect in Sect. 3.1. In view of this lack of systematic errors, we regard this as our best result, i.e. $3.7 \pm 1.1 \times 10^{-5}$ γ cm^{-2} s^{-1}, with a possible systematic error $\pm 0.3 \times 10^{-5}$ due to the non-uniform energy resolution.

The significance $\sim 3\sigma$ is rather better than that of Smith's (2004) result, $3.6 \pm 1.4 \times 10^{-5}$ γ cm^{-2} s^{-1}, but the agreement between the two is very good.

4. Discussion

In the context of massive star evolution, ^{26}Al comes from zones containing free protons (H and Ne burning) while ^{60}Fe requires a substantial free neutron abundance (C, Ne and to a small extent He burning). In the final supernova explosion, they will be produced in roughly equal amounts (Limongi & Chieffi 2003). Prantzos (2004) pointed out the contradiction between this expected CCSN ratio and results such as ours and Smith's (2004), where the ratio is $\sim$0.2. His conjecture that there is a large additional source of ^{26}Al which acts prior to the core collapse and explosion appears to be borne out by the models of Palacios et al. (2005), who find this source to be the massive winds expelled during the Wolf-Rayet (WR) phase. The key point is that there is a large abundance of ^{26}Al in H-burning layers which are close enough to the surface for the wind to expel it during the star's short presupernova life. The ^{60}Fe abundance is much further inside.

Surprisingly, therefore, the Galactic distributions of the ^{26}Al and ^{60}Fe lines may be quite different. WR stars differ from the average SNII progenitor in being (a) somewhat more massive on average and (b) highly dependent on metallicity. The ^{26}Al map exhibits "hot spots" in areas like Cygnus which are too young for even their most massive stars to have become SNII, but in which WR winds are already active (Knödlseder et al. 2002); ^{60}Fe emission should not be seen from these regions. The metallicity gradient in the Galaxy is substantial enough for excess ^{26}Al emission to be seen from the inner Galaxy in COMPTEL data (Palacios et al. 2005); ^{60}Fe should be more evenly distributed. When the possibility is factored in that some ^{60}Fe is made in SNIa (Iwamoto et al. 1999), and some ^{26}Al in AGB stars and novae (Diehl 2001), which have a quite different history and distribution, it appears that we must expect the unexpected when the data become sufficient for a ^{60}Fe map to be made.

Acknowledgements. The SPI project was completed under the responsibility and leadership of CNES. We are grateful to ASI, CEA, CNES, DLR, ESA, INTA, NASA and OSC for support.

References

Diehl, R. 2001, in The Universe in Gamma Rays, ed. V. Schönfelder (Berlin: Springer), 233
Harris, M. J., Purcell, W. R., McNaron-Brown, K., et al. 1997, in Proc. Fourth Compton Symp., ed. C. D. Dermer, M. S. Strickman, & J. D. Kurfess (New York: AIP), AIP Conf. Proc., 410, 1079
Hauser, M. G., Kelsall, T., Leisawitz, D., & Weiland, J. 1998, COBE Ref Pub. No. 98-A (Greenbelt, MD: NASA/GSFC), available in electronic form from the NSSDC
Iwamoto, K., Brachwitz, F., Nomoto, K., et al. 1999, ApJS, 125, 439
Knödlseder, J., Bennett, K., Bloemen, H., et al. 1999, A&A, 344, 68
Knödlseder, J., Cerviño, M., Le Duigou, J. M., et al. 2002, A&A, 390, 945
Knödlseder, J., Valsesia, M., Allain, M., et al. 2004, in The *INTEGRAL* Universe, ed. V. Schönfelder, G. Lichti, & C. Winkler (Noordwijk: ESA), ESA Special Publ., 552, 33
Knödlseder, J., Jean, P., Lonjou, V., et al. 2005, A&A, submitted
Limongi, M., & Chieffi, A. 2003, ApJ, 592, 404
Mahoney, W. A., Ling, J. C., Jacobson, A. S., & Lingenfelter, R. E. 1982, ApJ, 262, 742
Palacios, A., Meynet, G., Vuissoz, C., et al. 2005, A&A, 429, 613
Prantzos, N. 2004, A&A, 420, 1033
Smith, D. M. 2004, in The *INTEGRAL* Universe, ed. V. Schönfelder, G. G. Lichti, & C. Winkler (Noordwijk: ESA), ESA Special Publ., 552, 45 ≡ LANL preprint [arXiv:astro-ph/0404594]